Desalination and Water Treatment
www.deswater.com

doi: 10.5004/dwt.2019.23378

143 (2019) 29–37
March

Computational fluid dynamics (CFD) modeling of hydrocyclone for the recovery of ballasts and removal of sludge floc in ballasted flocculation process

Ki-Yeon Kim†, Seongjun Park†, Won-Hee Lee, Jong-Oh Kim*

Department of Civil and Environmental Engineering, Hanyang University, 222 Wangsimni-ro, Seongdong-gu, Seoul 04763, South Korea, Tel. +82 2 2220 0325; Fax: +82 2 2220 1945; email: jk120@hanyang.ac.kr (J.-Oh Kim), Tel. +82 2 2220 4512; emails: kimyeon072@naver.com (K.-Y. Kim), jayenv93@hanyang.ac.kr (S. Park), wheelwh@naver.com (W.-H. Lee)

Received 31 August 2018; Accepted 15 October 2018

ABSTRACT

The ballasted flocculation (BF) process is widely used in the water treatment process to cope with climate change. Microsand and magnetite are commonly used, which act as a seed in ballasted floc. The recovery of the ballast in BF process can affect the operating cost. In this study, we evaluate various sizes of magnetite particle with a specific gravity of above 5 in order to apply the hydrocyclone as a ballast recovery system in the BF process. The conventional purpose of the hydrocyclone is to separate solids and liquids, while the ideal recovery system in BF process should separate the ballast from the sludge and liquid. Computational fluid dynamics modeling was prepared to estimate the optimal conditions for the ballast recovery and the sludge removal ratio. The average ballast recovery ratio shows up to 99.9% varying with the inlet flow velocity. As the inlet flow velocity increases, the average sludge removal ratio decreases until 2 m/s, but it changes to increase after 2 m/s. The highest ratio is approximately 91% at 3.5 m/s of inlet flow velocity. This difference is due to the Reynolds number, which are summarized as the change of the particle size, the inlet flow velocity, and the specific gravity. In addition, the separation efficiency of each particle shows a fish-hook shape related with the Reynolds number. In BF process, the ballast recovery ratio should be maintained high, while the sludge recovery ratio should be maintained low. Criteria for the ballast and sludge recovery can be reached by maintaining the range of particle size, simultaneously satisfying this requirement at a certain inlet flow velocity. In other respects, for optimal ballast recovery and sludge removal, above a certain size of ballast should be used, and the sludge needs to be pulverized to a certain size as the pretreatment of the hydrocyclone.

Keywords: Ballasted flocculation; Hydrocyclone; Recovery of ballast; Sludge removal; Fish-hook phenomenon

1. Introduction

Currently, climate change makes great polarization impacts on the drought and flood season on natural water system, thus rapid and efficient technology responses are inevitable [1]. An importance of flocculation/sedimentation system is increasing, because the contaminant concentration increases during the dry season, and the high turbidity water frequently flows during the flood season [2]. As one of the solutions, ballasted flocculation (BF) processes are widely proposed [3], which are a technology that can increase the surface loading rate more than 40–100 times compared with the conventional process [4]. Ballasts, such as microsand and magnetite having a high specific gravity, act as a seed in ballasted flocs and increase the settling velocity of flocs [4,5]. The typical BF processes are composed with the mixing zone, the floc-settling zone and the ballast recovery zone. In the mixing zone, the raw water flows into the mixer, mixes with

* Corresponding author.
† Joint first authorship.

the ballast and the coagulant, and results in a ballasted floc. In the floc-settling zone, the various sedimentation systems have been adapted for the higher separation efficiency of the treated water and the flocs. Finally, the separated ballasted flocs are moved to the ballast recovery zone for further separation of the sludge and the ballast. The recovery system of the ballast requires a maximization of ballast recovery ratio and sludge rejection ratio, because those affect the operation cost and the treated water quality.

Because hydrocyclone has been used as the most suitable technology for separating particles, it also has been successfully adapted to recovery system in the BF processes [6–8]. The hydrocyclone is one of the most useful devices for separating particles by specific gravity difference. The fluid-containing particles feed the inlet, and vortex motion is occurred due to the internal structure. The particles of high specific gravity are separated along the wall to the descending underflow. On the other hand, the particles of small specific gravity are discharged to the overflow generated at the center of the hydrocyclone through the vortex finder. Therefore, the ballast with high specific gravity can be recovered, and the sludge with low specific gravity can be discharged [9,10]. The hydrocyclone has different separation efficiency depending on the change of the inlet flow velocity or the geometrical shape; therefore, these studies have been conducted according to the applied particles [11,12]. Park [13] showed the difference of the size and concentration of the discharged particles at the underflow according to the inlet flow velocity and concentration using a sediment with a specific gravity of 1.87–1.92. As a result, according to the increase of the inlet velocity, pollutants were less measured at the underflow than the particles were. Majumder et al. [14] conducted the similar experiment using a magnetite with a specific gravity of 1.35–1.45.

Although we understand that the efficiency of hydrocyclone is sensitive to change experimental conditions or geometrical design [15,16], all conditions and designs cannot be tested experimentally. Therefore, computational fluid dynamics (CFD) analysis can be the best alternative to understand the behavior of hydrocyclone in the BF process. Not only CFD analysis provides information on how complex fluid dynamics are affected by changes in geometry and initial conditions [17], but also it is possible to save cost and time, because it is free from change of analysis condition and modify the model [18].

In this study, we evaluate various sizes of magnetite particle with a specific gravity of above 5 in order to apply the hydrocyclone as a magnetite recovery system in the BF process. The conventional purpose of the hydrocyclone is to separate solids and liquids, while the ideal recovery system in BF process should separate the ballast from the sludge and liquid. Therefore, we evaluated the recovery ratio of magnetite ballast and the removal ratio of sludge using the CFD program with the change of inlet flow velocity and the ballast size.

2. Materials and methods

2.1. Basic geometry of the hydrocyclone

The hydrocyclone for both CFD modeling and experimental adjustment was designed with 20 mm of top diameter and 3.54 mm of underflow diameter. The involuted feed structure was applied to maximize the centrifugal force and to recover ballast and remove separated sludge as shown in Fig. 1. The structure of the feed inlet is important, because the area of feed inlet is closely related with the inlet flow velocity. The involuted feed structure was used to set the fluid to swirl when it is fed by the spiral structure and the narrowing inlet [19]. The area of the inlet determines the inlet flow velocity at the same inlet flow. The minimum cross-sectional area of the applied involuted feed structure is four times smaller than the inlet area, as a result, the inlet flow velocity is increased about four times, and the vortex motion by the structure is continued [11]. The underflow diameter was designed to maximize the overflow related with discharging the sludge. The detailed geometric design parameters of the hydrocyclone are summarized in Table 1.

2.2. CFD analysis

Flow-3D (Flow science, Inc., USA, v11.2) was used for the CFD analysis to model the hydrocyclone. The CFD analysis was conducted to seven cases ranging from 0.5 to 3.5 m/s at every 0.5 m/s interval. The mesh also can be generated with the Flow-3D program, and the normal mesh size is set to 0.5 mm. Because the inlet is narrowed by the involuted feed structure, the mesh size is applied by using the mesh plane. The number of mesh for the hydrocyclone is about 510,000. The turbulence model used in the analysis was a renormalized group (RNG) model. The RNG model has a constant empirically found and has broader applicability than other similar turbulence model [15,20,21]. To analyze

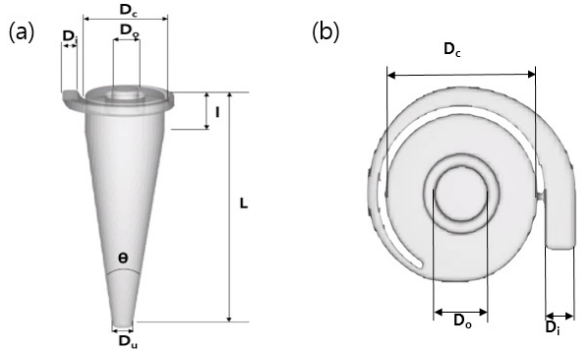

Fig. 1. Schematics of hydrocyclone: (a) geometry of the hydrocyclone and (b) involuted feed structure.

Table 1
Geometrical characteristics of hydrocyclone

Nomenclature		Value
D_c	Top diameter	20 mm
D_i	Inlet diameter	4 mm
L	Total length	80 mm
l	Vortex finder length	7 mm
D_o	Vortex finder diameter	6.9 mm
D_u	Underflow diameter	3.54 mm
Angle, θ	Cone angle	13°

the separation efficiency between magnetite and sludge in the hydrocyclone, magnetite with specific gravity of 5.57 was prepared as particle diameter of 20, 40, and 60 μm, while sludge with specific gravity of 1.06 was prepared as particle diameter of 20, 60, 100, and 200 μm. The detailed information on the CFD modeling is summarized in Fig. S1.

2.3. Experimental adjustment of the inlet flow velocity and the material properties

The more accurate CFD results can be obtained, and the more initial condition is set as in the actual condition [22,23]. The actual overflow and underflow ratio were measured from two outlets of the hydrocyclone according to the inlet flow velocity in the laboratory. According to the existing studies, the optimum inlet flow velocity of hydrocyclone was reported to be 1–3 m/s [24]. In the laboratory experiment, the condition of the inlet flow velocity was set at 0.5–3.5 m/s as used in CFD analysis.

The properties of the raw water flowing into the hydrocyclone were set similarly to the experimental conditions, which is preliminarily set up at pilot plant in South Korea (data not shown here). The raw water contains 3,000 mg/L of the ballast and 900 mg/L of sludge, and the manufactured magnetite is used as the ballast. The particle size distribution of the magnetite was measured using a particle size analyzer (Dandong Bettersize Instruments Ltd., Bettersize2000, China). Fig. 2 shows the particle distribution of the magnetite at the average particle size of 60 μm used in the actual coagulation–flocculation process. As shown in Fig. 2, 70% of the ballast of 60 μm or more, 30% of the ballast of 40 μm or less, and 5 % of the ballast of 20 μm or less are included. On the other hand, the mean particle size of the sludge is 200 μm. Because the sludge is expected to be crushed, the size of the sludge could be gradually smaller. Table 2 shows the estimated particle ratio, weights of each particle, and the calculated number of inlet particle applied to CFD analysis. In the same manner, all the values were calculated at the other inlet velocity and applied to CFD analysis as shown in Table S1.

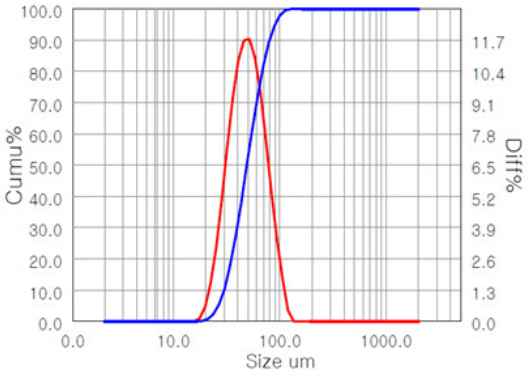

Fig. 2. Particle size distribution of 60 μm magnetite.

2.4. Estimation of mass balance and recovery ratio

Assuming no accumulation of mass in the hydrocyclone, the sum of the mass discharging the overflow and underflow of the hydrocyclone is equal to the inlet mass. Therefore, the inlet mass is conserved with the mass of the overflow and underflow as expressed in Eq. (1).

$$m = m_o + m_u \tag{1}$$

where m, m_o, and m_u are total mass in inlet flow, overflow mass, and underflow mass, respectively.

The recovery ratio of the particles (E_1) or the removal ratio of the particles (E_2) can be calculated as follows:

$$E_1 = \frac{m_u}{m_u + m_o} \quad \text{or} \quad E_2 = \frac{m_o}{m_u + m_o} \tag{2}$$

3. Results and discussion

3.1. Experimental property of the designed hydrocyclone

The overflow and underflow ratio measured from the experimental values was applied to the boundary condition in the CFD analysis condition. The actual experimental conditions are inlet flow velocity ranging from 1.5 to 3 m/s. The other over- and underflow ratios were calculated from the calibration curve through the experimental data, and the respective values are shown in Table 3. Table 3 shows the over- and underflow ratio by inlet flow velocity, and the underflow ratio decreases linearly according to the inlet flow velocity increases. The R^2 value (0.9994) of correlation between measured and calculated values was very close to 1 as shown in Fig. 3.

Table 2
Calculation of inlet particles at an inlet velocity of 2 m/s

Division	Concentration (mg/L)	Inlet flow rate (L/s)	Particle size (μm)	Specific gravity	Distribution of particles (%)	Weight of particle (mg/particle)	Number of inlet particles (particles/s)
Magnetite	3,000	0.025	60	5.57	70	6.3×10^{-4}	107,836
			40		25	1.9×10^{-4}	38,513
			20		5	2.3×10^{-5}	7,703
Sludge	900		200	1.06	25	4.4×10^{-3}	1,266
			100		25	5.6×10^{-4}	10,130
			60		25	1.2×10^{-4}	46,899
			20		25	4.4×10^{-6}	1,266,273

3.2. Average ballast recovery and sludge removal ratio by the inlet flow velocity

Fig. 4 shows CFD results of the ballast recovery ratio and the sludge removal ratio according to inlet flow velocity, which reflected the distribution and weight of the particles. It shows a high recovery ratio of 99% or more over 1 m/s of inlet flow velocity. At the inlet flow velocity of 2 m/s, the average ballast recovery ratio was 99.9%, which is the maximum. Because the tested ballasts have a high specific gravity of 5.57, even the velocity of 1.5 m/s was reported that can be affected by the centrifugal force, which shows the stable recovery ratio of 99% or more. In the case of the sludge removal, as the inlet flow velocity increases, the average sludge removal ratio decreases until 2 m/s, while it changes to increase after 2 m/s. The highest removal ratio is approximately 91% at 3.5 m/s of inlet flow velocity. This indicates that the separation characteristics of particles are different depending on the inlet flow velocity. Particularly, although the optimal inlet flow velocity is reported to be 1.5–3 m/s in the conventional hydrocyclone, the results show that the optimal inlet flow velocity is above 3 m/s for the BF process considering the sludge removal ratio.

3.3. Particle size affecting ballast recovery and sludge removal ratio

Fig. 5 shows the separation efficiency varying with particle size of the ballast and sludge. The larger size ballast shows the higher recovery ratio, while the larger size sludge shows the lower removal ratio. In comparison with Fig. 4, the large size particle leads the trend of the average ballast recovery ratio and sludge removal ratio. As shown in Table 2, because the large size ballast is composed with the high contents, the recovery trend of 60 μm ballast is very close to the average trend. In case of the sludge particle, because the distribution is relatively even, the trend of average values is similar to that of the heavier 100 and 200 μm particles but tends to be mitigated due to the trend of small size particles of 20 and 60 μm.

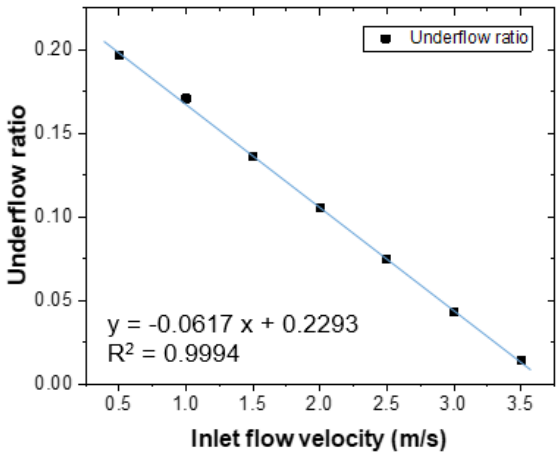

Fig. 3. Underflow ratio according to inlet flow velocity (underflow ratios are estimated at 0.5, 1, and 3.5 m/s based on the experimental data).

Table 3
Overflow and underflow ratio by inlet flow velocity

Division	Value						
Inlet flow velocity (m/s)	0.5	1	1.5	2	2.5	3	3.5
Inlet flow rate (m^3/d)	0.54	1.09	1.63	2.17	2.71	3.26	3.80
Overflow ratio	0.80	0.83	0.86	0.89	0.93	0.96	0.99
Underflow ratio	0.20	0.17	0.14	0.11	0.07	0.04	0.01

Note: The results of 1.5–3 m/s are experimentally measured.

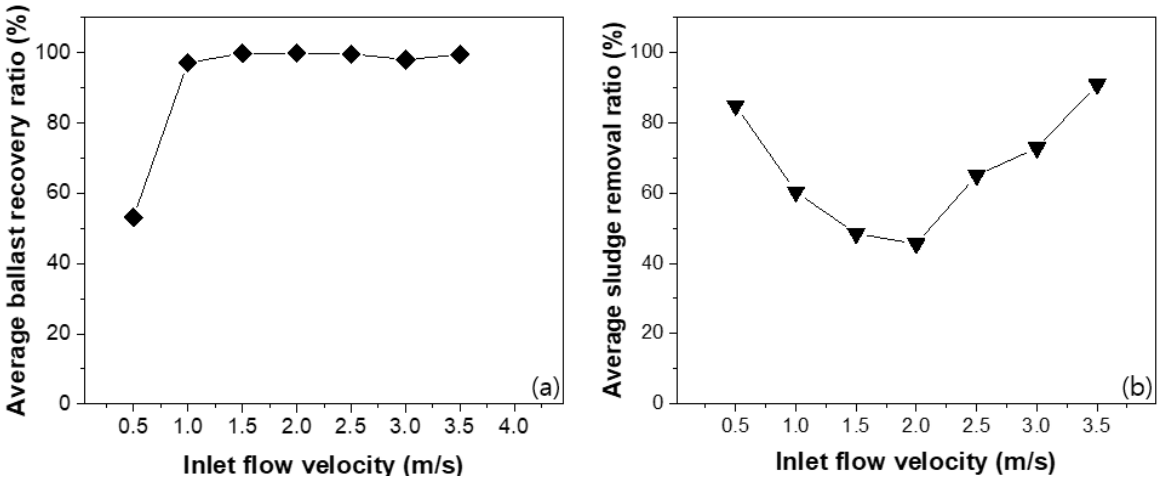

Fig. 4. CFD results by inlet flow velocity: (a) average ballast recovery ratio and (b) average sludge removal ratio.

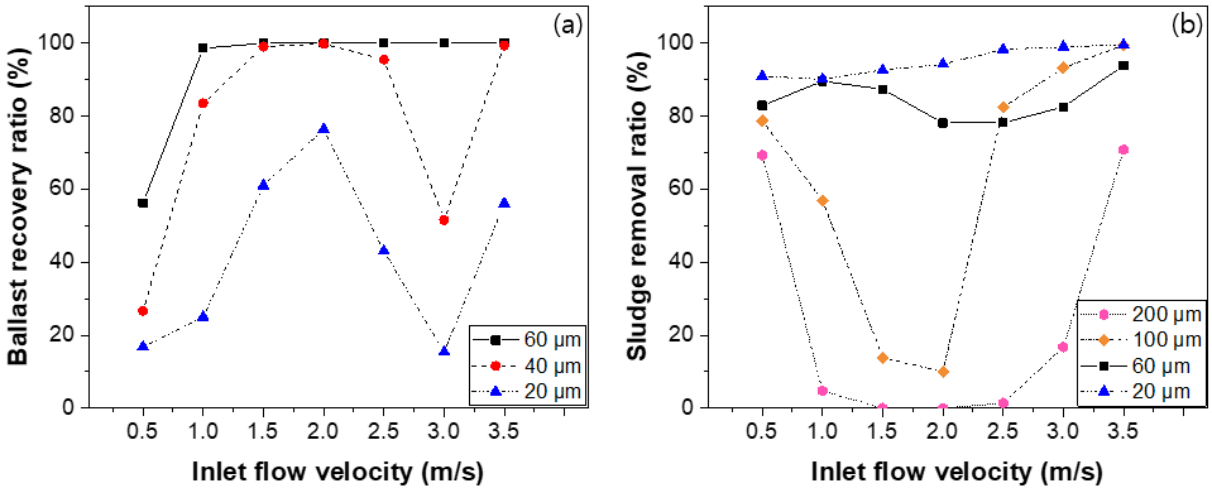

Fig. 5. CFD results by inlet flow velocity: (a) ballast recovery ratio and (b) sludge removal ratio.

40 and 60 μm ballast seems to show the optimal recovery ratio between 1.5 and 2.5 m/s, however, the recovery ratio increases again above 99% after suddenly dropping at 3.0 m/s. These specific curved patterns are repeatedly observed in the smaller sized ballast and sludge. The reason seems to be related with that the separation efficiency of each particle is influenced by the Reynolds number. Because the Reynolds number is expressed by the ratio of the inertia force to the viscous force as shown in Eq. (3), the inlet flow velocity and the particle size affect the inertia force of the particles.

$$\mathrm{Re} = \frac{\rho V L}{\mu} \sim \frac{\text{Inertia force}}{\text{Viscous force}} \tag{3}$$

where ρ is the density of fluid, V is the velocity of flow, L is the hydrocyclone diameter, and μ is the viscosity of fluid [25,26].

Majumder et al. [14] studied a fish-hook curve that shows the separation efficiency of particles depending on the influence of Reynolds number. When the experimental condition or geometry of hydrocyclone is changed, the intensity of centrifugal force is changed. Therefore, the particles in the hydrocyclone are affected differently according to Reynolds number, and the result represents "fish-hook" in various shapes [14].

3.4. Change of the fish-hook pattern by inlet flow velocity

Fish-hook phenomenon was analyzed with further CFD modeling under the conditions of inlet flow velocity of 2 m/s, which indicates the maximum ballast recovery ratio, and inlet flow velocity of 3.5 m/s, which indicates the maximum sludge removal ratio. Particle sizes from 1 to 200 μm were applied, and results were plotted based on the recovery ratio of the ballast and sludge as shown in Fig. 6. The "fish-hook" patterns were not observed at an inlet flow velocity of 2 m/s, and the ballast and sludge particle recovery ratio have stable separation characteristics. However, the "fish-hook" appeared at inlet flow velocity 3.5 m/s which seems to have reached the certain Reynolds number that can affect the recovery ratio. The sludge particles with low specific gravity have a clear fish-hook shape. Fig. 6(b) represents a critical point at 40 μm particle and a dip point at 100 μm particle, which is the particle size from which the recovery of relatively coarser particle in the underflow starts decreasing and the relatively coarser particle size where the recovery is minimum, respectively. The 110 μm of particle size shows the end point which is the same recovery ratio as the critical point [14]. The ballast with a higher specific gravity than sludge has relatively stable separation characteristic and shows a much smaller fish-hook pattern than that of sludge in between 15 and 40 μm.

In BF process, the ballast recovery ratio should be maintained high, while the sludge recovery ratio should be maintained low. For instance, if the criteria of ballast and sludge recovery ratios are above 80% and below 20%, respectively, the range of particle size simultaneously satisfying this requirement is 20–60 μm at inlet flow velocity of 2 m/s, while it is 40–105 μm at inlet flow velocity of 3.5 m/s. In other respects, the optimal ranges of the ballast and sludge size are above 40 μm and below 20 μm, respectively. Therefore, for optimal ballast recovery and sludge removal, a ballast of a certain size or more should be used, and the sludge needs to be pulverized to a certain size as the pretreatment of the hydrocyclone.

In comparison between Figs. 6(a) and (b), the ballast recovery was not significantly different when the inlet flow rate was increased above 40 μm, however, the recovery rate of sludge could be maintained low even at larger size. This could give us alternatives between the crushing energy saving and the pumping energy saving for increasing inlet velocity.

4. Conclusion

In this study, we evaluate various sizes of magnetite particle with a specific gravity of above 5 in order to apply the hydrocyclone as a magnetite recovery system in the BF process. The conventional purpose of the hydrocyclone is to separate solids and liquids, while the ideal recovery system in BF process should separate the ballast from the sludge and liquid. CFD modeling was prepared to estimate the optimal

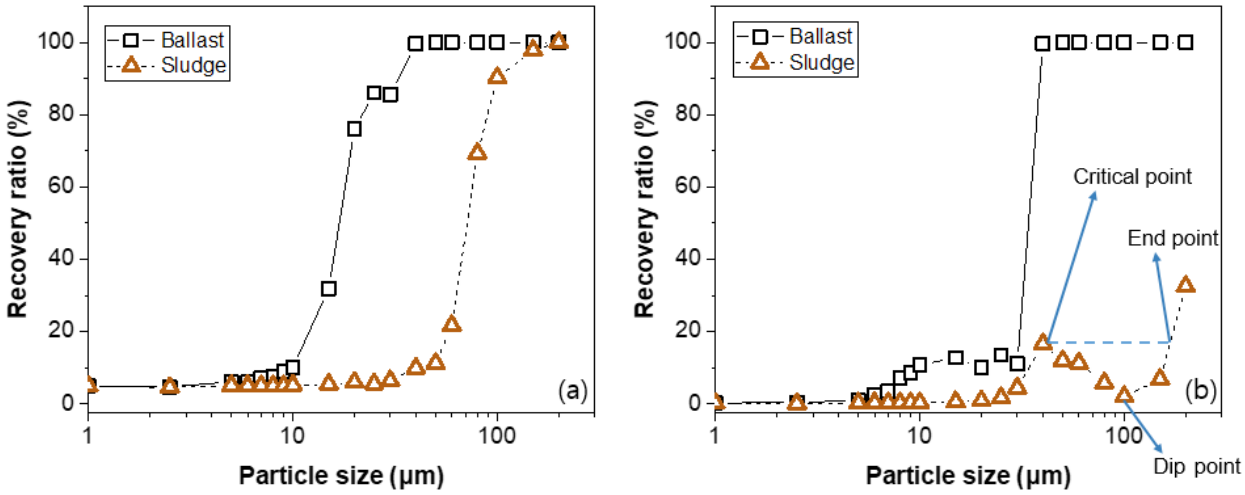

Fig. 6. Separation characteristics of ballast and sludge recovery ratio at underflow: CFD results at inlet flow velocity of (a) 2 m/s and (b) 3.5 m/s.

conditions for the ballast recovery and the sludge removal ratio. The average ballast recovery ratio shows up to 99.9% varying with the inlet flow velocity. As the inlet flow velocity increases, the average sludge removal ratio decreases until 2 m/s, but it changes to increase after 2 m/s. The highest ratio is approximately 91% at 3.5 m/s of inlet flow velocity. These differences are due to the Reynolds number which summarized the change of the particle size, the inlet flow velocity, and the specific gravity. In addition, the separation efficiency of each particle shows a fish-hook shape related with the Reynolds number. In BF process, the ballast recovery ratio should be maintained high, while the sludge recovery ratio should be maintained low. Criteria for the ballast and sludge recovery can be reached by maintaining the range of particle size simultaneously satisfying this requirement at a certain inlet flow velocity. In other respects, for optimal ballast recovery and sludge removal, above a certain size of ballast should be used, and the sludge needs to be pulverized to a certain size as the pretreatment of the hydrocyclone.

Acknowledgment

This subject is supported by Korea Ministry of Environment as "Global Top Project (2016002110006)".

References

[1] S. Park, Y. Moon, J.O. Kim, Evaluation of the image analysis method using statistics for determining the floc size and settling velocity in ballasted flocculation, Desal. Wat. Treat., 99 (2017) 220–227.
[2] I. Delpla, A.V. Jung, E. Baures, M.C. Lement, O. Thomas, Impacts of climate change on surface water quality in relation to drinking water production, Environ. Int., 35 (2009) 1225–1233.
[3] C. Desjardins, B. Koudjonou, R. Desjardins, Laboratory study of ballasted flocculation, Water Res., 36 (2002) 744–754.
[4] J.C. Young, F.G. Edwards, Fundamentals of ballasted flocculation reactions, Proc. Water Environ. Fed., 14 (2000) 56–80.
[5] C. Cailleaux, E. Pujol, F.D. Dianous, J. Drouton, Study of weighted flocculation in view of a new type of clarifier, J. Water Supply Res. Technol. AQUA, 41 (1992) 18–27.
[6] K.H. Kwon, S.W. Kim, L.H. Kim, J.H. Kim, S. Lee, K.S. Min, Particle removal properties of stormwater runoff with a lab-scale vortex separator, Desal. Wat. Treat., 38 (2012) 301–305.
[7] W. Kurtz, J.G. Muller, A. Laurence, R.D. Smith, P.J. Young, Pilot testing of high rate physical-chemical treatment (HRPCT) for wet weather treatment, Proc. Water Environ. Fed., 8 (2003) 452–464.
[8] J.P. O'Hare, T. Perry, Investigating treatment options to meet a 70 ug/L phosphorus discharge limit for the Boise River in Idaho, Proc. Water Environ. Fed., 16 (2010) 908–913.
[9] J. Cullivan, R. Williams, T. Dyakowski, C. Cross, New understanding of a hydrocyclone flow field and separation mechanism from computational fluid dynamics, Miner. Eng., 17 (2004) 651–660.
[10] S. Kawatra, A. Bakshi, M. Rusesky, The effect of slurry viscosity on hydrocyclone classification, Int. J. Miner. Process., 48 (1996) 39–50.
[11] L.-Y. Chu, W.-M. Chen, X.-Z. Lee, Effect of structural modification on hydrocyclone performance, Sep. Purif. Technol., 21 (2000) 71–86.
[12] M. Fisher, R. Flack, Velocity distributions in a hydrocyclone separator, Exp. Fluids, 32 (2002) 302–312.
[13] J.H. Park, Separation of Reservoir Sediment by Using Hydrocyclone, Kyunghee University, Korea, 2002.
[14] A. Majumder, H. Shah, P. Shukla, J. Barnwal, Effect of operating variables on shape of "fish-hook" curves in cyclones, Miner. Eng., 20 (2007) 204–206.
[15] M. Azadi, M. Azadi, A. Mohebbi, A CFD study of the effect of cyclone size on its performance parameters, J. Hazard. Mater., 182 (2010) 835–841.
[16] K.W. Chu, B. Wang, A.B. Yu, A. Vince, CFD-DEM modelling of multiphase flow in dense medium cyclones, Powder Technol., 193 (2009) 235–247.
[17] W.P. Martignoni, S. Bernardo, C.L. Quintani, Evaluation of cyclone geometry and its influence on performance parameters by computational fluid dynamics (CFD), Braz. J. Chem. Eng., 24 (2007) 83–94.
[18] B. Wang, K. Chu, A. Yu, Numerical study of particle–fluid flow in a hydrocyclone, Ind. Eng. Chem. Res., 46 (2007) 4695–4705.
[19] F. Ntengwe, L.K. Witika, Optimization of the operating density and particle size distribution of the cyclone overflow to enhance the recovery of the flotation of copper sulphide and oxide minerals, J. S. Afr. Inst. Min. Metall., 111 (2011) 295–300.
[20] C.G. Speziale, S. Thangam, Analysis of an RNG Based Turbulence Model for Separated Flows, Institute for Computer Applications in Science and Engineering, NASA Langley Research Center, 1992. Available at: https://ntrs.nasa.gov/search.jsp?R=19920010431.

[21] W.D. Griffiths, F. Boysan, Computational fluid dynamics (CFD) and empirical modelling of the performance of a number of cyclone samplers, J. Aerosol Sci., 27 (1996) 281–304.
[22] M.E. Nnacer, G. Guevremont, T. Djeridane, S. Sreekanth, T. Lucas, Blade Air Cooling Feed System CFD Analysis and Validation, ASME Turbo Expo 2007: Power for Land, Sea, and Air, American Society of Mechanical Engineers, 2007, pp. 1171–1180.
[23] M. Nijemeisland, A.G. Dixon, Comparison of CFD simulations to experiment for convective heat transfer in a gas–solid fixed bed, Chem. Eng. J., 82 (2001) 231–246.
[24] H. Yurdem, V. Demir, A. Degirmencioglu, Development of a mathematical model to predict clean water head losses in hydrocyclone filters in drip irrigation systems using dimensional analysis, Biosyst. Eng., 105 (2010) 495–506.
[25] Z.-S. Bai, H.-L. Wang, Crude oil desalting using hydrocyclones, Chem. Eng. Res. Design, 85 (2007) 1586–1590.
[26] Z.S. Bai, H.L. Wang, S.T. Tu, Removal of catalyst particles from oil slurry by hydrocyclone, Sep. Sci. Technol., 44 (2009) 2067–2077.

Supplementary materials

Table S1
Calculation of inlet particles by an inlet velocity

Inlet flow velocity (m/s)	Division	Concentration (mg/L)	Inlet flow rate (L/s)	Particle size (μm)	Specific gravity	Distribution of particles (%)	Weight of particle (mg/particle)	Number of inlet particles (particles/s)
0.5	Magnetite	3,000	0.006	60	5.57	70	6.3×10^{-4}	26,981
				40		25	1.9×10^{-4}	9,636
				20		5	2.3×10^{-5}	1,927
	Sludge	900		200	1.06	25	4.4×10^{-3}	317
				100		25	5.6×10^{-4}	2,535
				60		25	1.2×10^{-4}	11,734
				20		25	4.4×10^{-6}	316,820
1	Magnetite	3,000	0.013	60	5.57	70	6.3×10^{-4}	54,133
				40		25	1.9×10^{-4}	19,333
				20		5	2.3×10^{-5}	3,867
	Sludge	900		200	1.06	25	4.4×10^{-3}	636
				100		25	5.6×10^{-4}	5,085
				60		25	1.2×10^{-4}	23,543
				20		25	4.4×10^{-6}	635,659
1.5	Magnetite	3,000	0.019	60	5.57	70	6.3×10^{-4}	80,985
				40		25	1.9×10^{-4}	28,923
				20		5	2.3×10^{-5}	5,785
	Sludge	900		200	1.06	25	4.4×10^{-3}	951
				100		25	5.6×10^{-4}	7,608
				60		25	1.2×10^{-4}	35,221
				20		25	4.4×10^{-6}	950,966
2	Magnetite	3,000	0.025	60	5.57	70	6.3×10^{-4}	107,836
				40		25	1.9×10^{-4}	38,513
				20		5	2.3×10^{-5}	7,703
	Sludge	900		200	1.06	25	4.4×10^{-3}	1,266
				100		25	5.6×10^{-4}	10,130
				60		25	1.2×10^{-4}	46,899
				20		25	4.4×10^{-6}	1,266,273
2.5	Magnetite	3,000	0.031	60	5.57	70	6.3×10^{-4}	134,903
				40		25	1.9×10^{-4}	48,180
				20		5	2.3×10^{-5}	9,636
	Sludge	900		200	1.06	25	4.4×10^{-3}	1,584
				100		25	5.6×10^{-4}	12,673
				60		25	1.2×10^{-4}	58,670
				20		25	4.4×10^{-6}	1,584,102
3	Magnetite	3,000	0.038	60	5.57	70	6.3×10^{-4}	161,969
				40		25	1.9×10^{-4}	57,846
				20		5	2.3×10^{-5}	11,569
	Sludge	900		200	1.06	25	4.4×10^{-3}	1,901
				100		25	5.6×10^{-4}	15,215
				60		25	1.2×10^{-4}	70,442
				20		25	4.4×10^{-6}	1,901,932

(*Continued*)

Table S1 (*Continued*)

Inlet flow velocity (m/s)	Division	Concentration (mg/L)	Inlet flow rate (L/s)	Particle size (μm)	Specific gravity	Distribution of particles (%)	Weight of particle (mg/particle)	Number of inlet particles (particles/s)
3.5	Magnetite	3,000	0.044	60	5.57	70	6.3×10^{-4}	188,950
				40		25	1.9×10^{-4}	67,482
				20		5	2.3×10^{-5}	13,496
	Sludge	900		200	1.06	25	4.4×10^{-3}	2,219
				100		25	5.6×10^{-4}	17,750
				60		25	1.2×10^{-4}	82,176
				20		25	4.4×10^{-6}	2,218,752

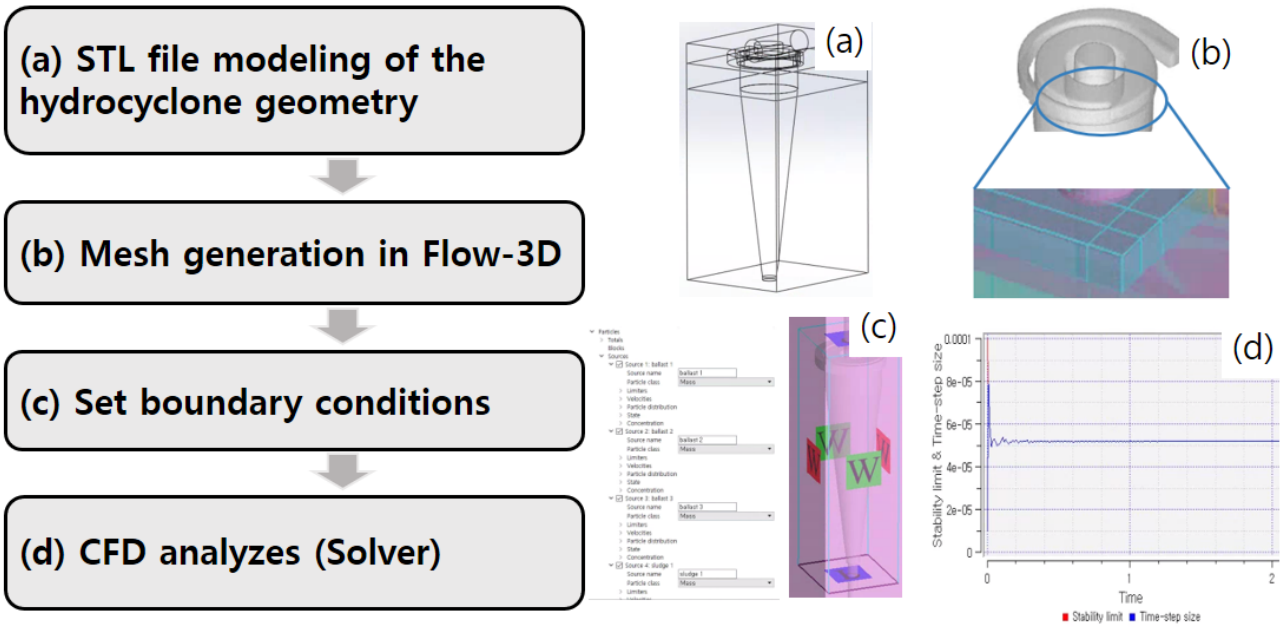

Fig. S1. CFD analysis using Flow-3D (Flow Science, Inc., USA, v11.2): (a) producing stereolithography (STL) file using modeling program, (b) mesh generation using mesh plane by Flow-3D quick tool, (c) setting boundary conditions in Flow-3D, and (d) solution and calculated values